

**Quasi Static Axial Loading on Carbon fiber wind to HDPE Composite Pipe
(CFWHCP)**

by

Chow Xuan Hui

16765

Dissertation submitted in partial fulfilment of
the requirements for the
Bachelor of Engineering (Hons)
(Mechanical)

MAY 2015

Universiti Teknologi PETRONAS
32610 Bandar Seri Iskandar
Perak Darul Ridzuan

CERTIFICATION OF APPROVAL

Quasi Static Axial Loading on Carbon fiber wind to HDPE Composite Pipe (CFWHCP)

by

Chow Xuan Hui

16765

A project dissertation submitted to the
Mechanical Engineering Programme
Universiti Teknologi PETRONAS
in partial fulfilment of the requirement for the
BACHELOR OF ENGINEERING (Hons)
(MECHANICAL)

Approved by,

(ASSOC. PROF. IR DR HAMDAN HAJI YA)

UNIVERSITI TEKNOLOGI PETRONAS
TRONOH, PERAK

May 2015

CERTIFICATION OF ORIGINALITY

This is to certify that I am responsible for the work submitted in this project, that the original work is my own except as specified in the references and acknowledgements, and that the original work contained herein have not been undertaken or done by unspecified sources or persons.

CHOW XUAN HUI

ABSTRACT

Carbon fiber-reinforced polymer, also known as carbon fiber-reinforced plastic is a type of composite polymer which is extremely strong and light. Manufacturers will select to use this material on high-end quality products such as exotic sports car, oil and gas equipment, aerospace and so on when there is a need of high strength-to-weight ratio specification. This project discusses on the fabrication of different arrangement of various sizes of carbon fiber tow wind to HDPE composite pipe (CFWHCP) and their mechanical properties. 2 types of sample with winding angle of 57° : CFWHCP of 6 fiber tows of same size (12k) and different size (12k and 6k); were fabricated with epoxy as the matrix in SIRIM Permatang Pauh. No fiber triangle potential voids of the samples were studied through SEM analysis. It was found that the no-fiber triangle void for 12k and 6k sample is larger than 12k sample. This is due to the arrangement of fiber tow which will be discussed more in problem statement in chapter 1.2. Literature review in chapter 2.2 proved that void content is inversely proportional to the mechanical strength of material. Through result analysis in dog-boned tensile test, hoop tensile test, axial & lateral quasi static loading test in chapter 3.2.5, it is proven that 12k sample with smaller void is better and higher in terms of failure mode, energy absorption and Young's modulus.

ACKNOWLEDGEMENT

I would like to express my deepest gratitude to my supervisor, AP Ir Dr Hamdan Haji Ya for providing me this great opportunity to embark on this project under his supervision. I sincerely appreciate all the guidance which has been offered by AP Ir Dr Hamdan Haji Ya along the way of completing this project. I had able to gain more knowledge on the project through all the experiences shared by AP Ir Dr Hamdan Haji Ya.

Next, I would like to thank all the technicians in UTP as well as in SIRIM Permatang Pauh which lend their helpful hand by the time I needed their help and guidance, especially the fabrication and testing process. No doubt that my project had able to flow smoothly with the helps that they had offered.

Last but not least, I wish to thank my beloved family for their never ending support that helps me push through to complete this project. Thank you.

TABLE OF CONTENTS

CERTIFICATION OF APPROVAL	ii
CERTIFICATION OF ORIGINALITY	iii
ABSTRACT	iv
ACKNOWLEDGEMENT	v
LIST OF FIGURES	vii
LIST OF TABLES	ix
CHAPTER 1: INTRODUCTION	1
1.1 Background	1
1.2 Problem Statement	3
1.3 Objectives and Scope of Study	4
CHAPTER 2: LITERATURE REVIEW	5
2.1 Composite Material.....	5
2.2 Carbon Fiber-Reinforced Polymer	6
2.3 Epoxy Resin as Matrix/.....	9
2.4 Filament Winding Technique	12
2.5 Quasi Static Axial Loading	15
2.6 Application of FRP in Oil and Gas Industry	17
2.7 Past Research on Quasi-Static Test	19
CHAPTER 3: METHODOLOGY	20
3.1 Process Flow	20
3.2 Research Methodology	22
3.3 Gantt Chart & Key Milestone.....	46
CHAPTER 4: CONCLUSION & RECOMMENDATION	47
4.1 Conclusion.....	47
4.2 Recommendation	48
REFERENCES	49
APPENDIX	51

LIST OF FIGURES

- Figure 1: Cross-section of carbon fiber (similar fiber tow)
- Figure 2: Cross-section of carbon fiber (varies fiber tow)
- Figure 3: Sample 12K carbon fiber tow
- Figure 4: Young's modulus of composites against void content
- Figure 5: Stress-strain curves of different volume fraction of fiber
- Figure 6: Idealized chemical structure of a typical epoxy
- Figure 7: Epoxy resin and liquid hardener chemical
- Figure 8: Resin bath machine
- Figure 9: Cure oven for epoxy curing process
- Figure 10: Customized filament winding machine in SIRIM Permatang Pauh
- Figure 11: Helical winding process
- Figure 12: CFWHCP wind at 57°
- Figure 13: Universal testing machine as static loading device
- Figure 14: Project Process Flow Chart
- Figure 15: Holder jig
- Figure 16: Straightener jig
- Figure 17: Hoop internal jig
- Figure 18: Hoop external jig
- Figure 19: CFWHCP sample for SEM test
- Figure 20: SEM result for six 12K fiber tows arrangement
- Figure 21: SEM result for two 12K + four 6K fiber tows arrangement
- Figure 22: Before & after boring process
- Figure 23: Dog-bones shape specimen for tensile test
- Figure 24: O-ring shape specimen for tensile test
- Figure 25: Original pipe specimen in axial position for compression test
- Figure 26: Original pipe specimen in lateral position for compression test
- Figure 27: Dog-bone tensile sample
- Figure 28: Dog-bone tensile stress-strain graph
- Figure 29: Hoop tensile sample

Figure 30: Hoop tensile Stress-Strain graph

Figure 31: top view (axial position compression test)

Figure 32: side view (axial position compression test)

Figure 33: Axial compression test load-displacement graph

Figure 34: Peak load comparison with past research samples

Figure 35: top view (lateral position compression test)

Figure 36: side view (lateral position compression test)

Figure 37: Lateral compression test load-displacement graph

LIST OF TABLES

Table 1: Result for SEM test

Table 2: Results for dog-boned tensile test

Table 3: Results for hoop tensile test

Table 4: Results for quasi static compression test (axial position)

Table 5: Results for quasi static compression test (lateral position)

CHAPTER 1

INTRODUCTION

1.1 BACKGROUND

In this modern era, automotive, construction and industrial field has such a high demand due to the increasing human population. This has subsequently increased the demand of high quality material having superior characteristic such as high strength-to-weight ratio, high fatigue strength, high corrosion resistance, low impact resistance and more. Conventional materials like steel and aluminum has failed to service due to the limitation of benefits they can provide. Industry has then starts to recognize the capability of composite materials in producing durable and high quality products.

One of the widely recognized high quality composite materials is carbon fiber reinforced polymers. CFRP can be expensive due to the usage of carbon fiber but are widely used wherever high strength-to-weight ratio and rigidity are required, such as high performance automotive industry and high strength and corrosion resistance oil & gas piping industry applications. Besides, this material is durable at the same time having high energy absorption and impact resistant.

The mechanical properties of CFRP is highly dependent on the proportions of carbon fiber and epoxy resin, orientation of carbon fiber, types of epoxy resin, sizes of carbon fiber, length of carbon fiber for discontinuous carbon fiber and void content [1]. In this project, the main interest focus on the relationship between different sizes of carbon fiber tow arrangement being wind onto high density polyethylene pipe (HDPE) and how their level of tolerance towards tension and compression test can be altered.

Filament winding technique is the technique that will be used in this project to wind the high density polyethylene pipe with carbon fiber to enhance the mechanical properties as well as great reduction of weight of the composite material. Throughout the project, winding tension, winding angle, resin content and winding layer will be fixed. The only changing variable is the usage of different sizes of carbon fiber in different specimens. It is noticed that by using similar sizes of fiber tow, it will form triangle at every crossing part which will produce voids and affect the mechanical properties of the composite materials. Voids can be reduced by introducing varies sizes of fiber tow of different bandwidth. This will thus enhanced the mechanical properties of the composite materials.

This project will investigate how different sizes of carbon fiber tow arrangement can affect the level of enhancement of mechanical properties on the composite pipe. Instead of similar size of fiber tow being introduced, different sizes of fiber tow will be used in the winding process for different specimens. Experiment results including mode of failure, energy absorption and Young's modulus will be determined and recorded.

1.2 PROBLEM STATEMENT

The optimum number of fiber tow to be used in filament winding process range from 5 to 8. In this project, the interest fiber tows are 6K and 12K which are the common bundle sizes used in market. The problem in this situation is that by using different sizes of fiber tow, there will be small gap formed at the end of every crossing part which will lead to the forming of no fiber triangle potential void when the material is cured. Although the void will later be filled up by matrix, the strength of the composite material will never achieve an optimum condition. This will subsequently affect the mechanical properties of high density polyethylene wind with carbon fiber composite pipe (CFWHCP). Figure 1 shows the cross section of carbon fiber reinforced polymer with smaller voids when wind using same sizes of fiber tows. In this project, it refers to 6 tows of 12K carbon fibers.

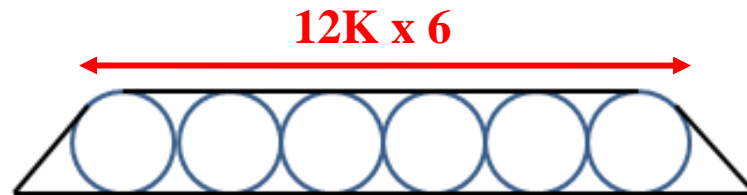


Figure 1: Cross-section of carbon fiber (similar fiber tow)

However, size of no fiber triangle potential void increase when different sizes of fiber tows are introduced, as shown in figure 2. Through figure 2 we can see that by using less number of carbon fibers, the void forming area at both ends will increase and eventually reduced the mechanical properties of CFWHCP. In this project, it refers to 2 tows of 12K carbon fibers + 4 tows of 6K carbon fibers.

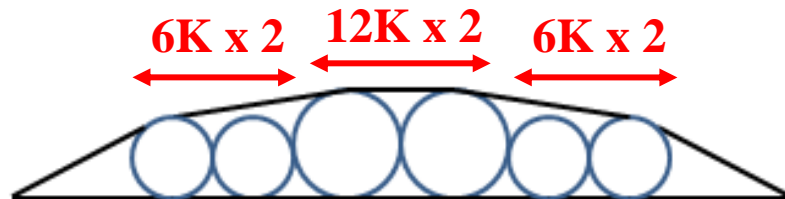


Figure 2: Cross-section of carbon fiber (varies fiber tow)

1.3 OBJECTIVES & SCOPE OF STUDY

The objective of this project:

- i. To investigate how different sizes of carbon fiber tow arrangement winding on high density polyethylene pipe can affect the level of enhancement of mechanical properties on the composite pipe
- ii. To study impact of quasi static axial loading on carbon fiber wind to high density polyethylene composite pipe (CFWHCP)

The scope of study of this project:

- i. Tackle the issue of no fiber triangle potential void for CFWHCP to enhance its mechanical properties
- ii. Analyze the results of stress-strain graph from tension test and load-displacement graph from compression test on carbon fiber wind to high density polyethylene composite pipe (CFWHCP)
- iii. Analyze the failure mode ,energy absorption and Young's modulus on carbon fiber wind to high density polyethylene composite pipe (CFWHCP) based on experiment results obtained

CHAPTER 2

LITERATURE REVIEW

2.1 COMPOSITE MATERIAL

A composite material or composites is made by combining two or more materials, often ones that having different properties. The two materials work together to give the composite unique properties in order to create material which is better in every aspect. Composite materials are made up of individual materials referred to as constituent materials [2]. There are two main categories of constituent materials, namely the matrix and the reinforcement. The matrix material surround, binds and supports the reinforcement materials by maintaining their positions [3]. The reinforcements provide their special mechanical and physical properties to enhance the matrix properties of new material being created. Reinforcement materials usually have very high tensile and compressive strength. But, these theoretical values cannot be achieved in structural form. The reasons may be due to presence of impurities or surface flaws during processing, which will eventually leads to formation of cracks. Strength of composite materials is thus affected [4].

Continuous development of technologies had offered way to overcome this problem that is to manufacture the reinforcement materials in fiber form. This will help to solve the crack formation issue which occurred previously. In order to make this happen, a matrix needed to be used to hold these fibers together and improve the material properties in the transverse direction of the fiber. Composite materials are commonly classifies based on the types of matrix involved. They can either be polymer, metallic or even ceramic. Besides acting as the fiber holder, matrix also plays an important role to protect the fiber from damage caused by temperatures or corrosion. Matrix also helps to spread the load equally to each individual fiber.

2.2 CARBON FIBER REINFORCED POLYMER

Carbon fiber reinforced polymer (CFRP) is a composite material made of polymer matrix reinforced with carbon fiber. CFRP are commonly used in automotive, aerospace as well as oil and gas industries. In this project, carbon fiber as reinforcement is wind to HDPE composite pipe (CFWHCP). CFWHCP consist of high modulus reinforcing carbon fibers embedded in a low modulus polymeric matrix. The combination of two different phases allows the load to be transferred between carbon fibers due to the elasticity in the matrix. The matrix serves to separate and protect the carbon fibers layer. Figure 3 shows the real carbon fiber sample taken from SIRIM Permatang Pauh before the winding process.

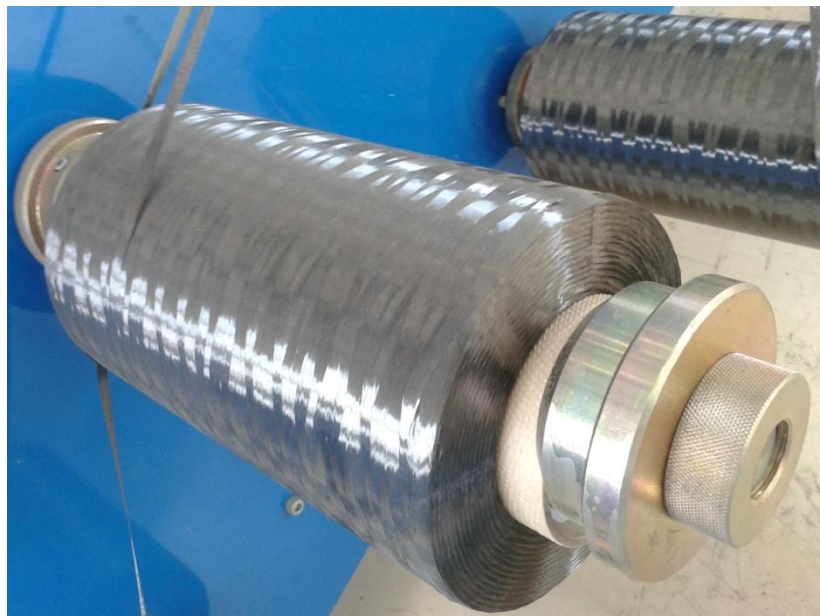


Figure 3: Sample 12K carbon fiber tow

Stiffness and strength of CFWHCP is very much depends on the proportions of carbon fiber, distribution and orientation of carbon fiber layers, sizes of carbon fiber tow and length of carbon fiber for discontinuous fiber and void content [5]. In this project, void content is very significant in determining the stiffness and strength of CFWHCP.

An investigation on random-chopped fiber reinforced polymer (FRP) composites containing high volume fraction of air voids shows that higher volume fraction of voids leads to a lower effective stiffness of the composites [6]. Figure 4 shows Young's modulus of composites against void content graph where Young's modulus decreases with the increasing of void content. Figure 5 shows the stress-strain curves of different volume fraction of fiber where tensile strength increases with the increment of fiber content.

According to the study by Zhang et al on the tensile strength of hydrothermally conditioned carbon fiber composites with voids, the results proved that the rate of water uptake increases when void increases. Besides, data shows that tensile strength of non-aged specimens decreased by 0.8% with void content range from 0.33% to 1.5%. This data clearly support the facts that tensile strength decreases when the amount of void content increases [7].

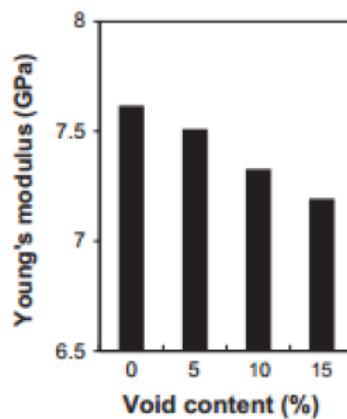


Figure 4: Young's modulus of composites against void content

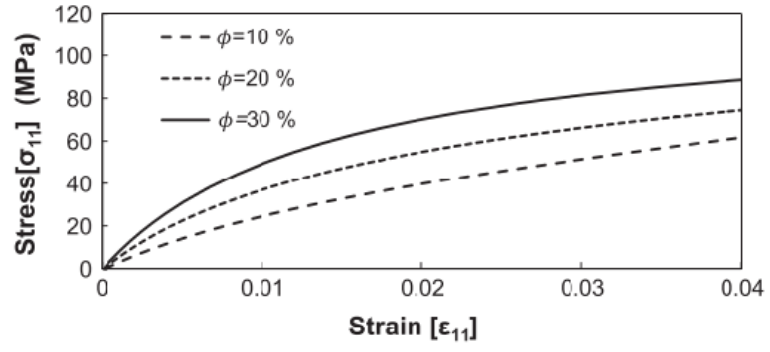


Figure 5: Stress-strain curves of different volume fraction of fiber

2.3 EPOXY RESIN AS THE MATRIX

To bind carbon fiber onto polymers, there are three types of resins used in today's manufacturing field. They are separately epoxy resin, vinyl ester and polyester resins. Each of them has their own different characteristics. Among the three, epoxy resin is chosen as the matrix in this project. Although, it is the most expensive among all three but well worth the cost. Epoxy resins are typically three times stronger than the other two resin types. It adheres very well to carbon fiber and forms a virtually leak-proof barrier [8]. Besides, the ability of epoxy to adhere well to older epoxy and most materials is also the reason why it is chosen for this project. Epoxy resins are easily and quickly cured at any temperature from 5°C to 150°C. Low shrinkage of epoxy resin during cure also helps to minimize fabric internal stresses.

The term 'epoxy' is a chemical group that consists of two carbon atoms bonded to an oxygen atom. Epoxy resins are formed from a long chain molecular structure with reactive sites at either end. These reactive sites are formed by epoxy groups instead of ester groups. Good water resistance of epoxy resin is due to the absence of these ester groups. The epoxy molecule also contains two ring groups at its center which are able to absorb both mechanical and thermal stresses better than linear groups and therefore give the epoxy resin very good stiffness, toughness and heat resistant properties [9].

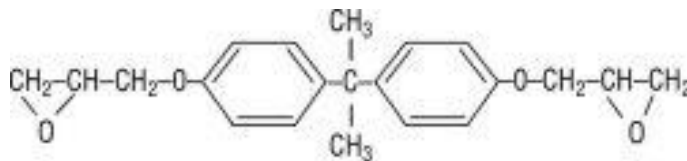


Figure 6: Idealized chemical structure of a typical epoxy

Figure 7 shows the separate content of epoxy resin and liquid hardener taken at SIRIM Permatang Pauh before they are mix. 57% epoxy resin mix with 43% liquid hardener, mixture were stir using machine for 10 minutes before pour into resin bath machine.



Figure 7: Epoxy resin and liquid hardener chemical

Figure 8 shows resin bath machine taken at SIRIM Permatang Pauh. Five tow of carbon fiber will pass through this machine, all deep soak with epoxy resin before wind onto HDPE composite pipe.



Figure 8: Resin bath machine

After carbon fiber complete the winding process, the whole specimen will undergo curing process inside cure oven for 3 hours before it is complete as the final product of CFWHCP.



Figure 9: Cure oven for epoxy curing process

2.4 FILAMENT WINDING TECHNIQUE



Figure 10: Customized filament winding machine in SIRIM Permatang Pauh

Filament winding technique is one of the processes of winding carbon fiber and resin around mandrel (HDPE composite pipe in this project) to create composite product. It is a process by which continuous reinforcing carbon fibers are accurately positioned in a predetermined pattern following the shape of cylindrical HDPE composite pipe.

During winding process, there are some parameters that can be varied, which are winding tension, winding angle and resin content in each layer of reinforcement. This is to ensure desired thickness and strength of the composite is achieved. The properties of the finished composite can be varied by the type of winding pattern selected. There are three filament winding patterns: circumferential winding, helical winding and polar winding. In this project, helical winding is chosen as it is the most common winding technique used in piping and vessels.



Figure 11: Helical winding process

It is very crucial to find the optimum winding angle for filament winding. Netting analysis is one of the attempts to optimize composite tubular structures. This technique assumes that fibers supported all loads, neglecting the contribution of the matrix and the interaction between the fibers. The optimum angle obtained from this technique which is 54.74° is normally used to manufacture composite tubular structures under close-end loading condition [10].

There are reasons why filament winding is preferred over other techniques. First is the ability of this technique to make very thin-walled products in relation to their diameter. It can provide an optimal balance between tensile strength, hoop strength and torsion resistance, which in combination with a high fiber tension when applying the filaments, results in a relatively thin walled product. Filament winding also gives consistent product quality due to the highly automated nature of the process. The tension of the filaments, and the epoxy resin/carbon fiber proportion are computer controlled, to a much higher degree of consistency than a human operator could. This leads to less variation in wall thickness and straightness in the finished products [11].

In this project, 57° has been selected as the best winding angle based on experimental studies develop through several specimen wind with different angle. 57° able to offer the best coverage area for HDPE composite pipe compared to other tried angle. Figure 12 shows the end products of HDPE being wind with carbon fiber at 57° .



Figure 12: CFWHCP wind at 57°

2.5 QUASI-STATIC AXIAL LOADING

Quasi-static loading refers to loading where inertial effects are negligible. In other words time and inertial mass are irrelevant. In quasi-static axial loading experiment, loading is applied in a very slow motion in one direction (monotonic) [12].



Figure 13: Universal testing machine as static loading device

Quasi-static loads are useful in determining the maximum allowable loads on engineering structures, such as bridges, and they can also be useful in discovering the mechanical properties of materials. This force is often applied to engineering structures that people's safety depends on because engineers need to know the maximum force a structure can support before it will collapse.

Any force applied steadily without moving an object is considered a static load and the knowledge of how much loading a structure can handle is useful for setting safety margins for the structure. Limiting the loading to one half of a structure's maximum will give a factor of safety of two.

Materials themselves can be subjected to a test to discover their fundamental properties. All materials have an intrinsic limit on how much tension or compression stress they can tolerate before yielding or permanently deforming. Stress is a measure of force per unit area in a material's cross section, and when the force per unit area becomes too great, microscopic fractures develop. If the force continues to rise, the material can break altogether.

Tensile test is performed in which a sample is subjected to a controlled tension until failure [13]. The results from the test are commonly used to predict how a material will react under other types of forces (in this project refers to high carbon fiber wind to HDPE composite pipe, CFWHCP). Properties that are directly measured via a tensile test are ultimate tensile strength, maximum elongation and reduction in area. Young's modulus, Poisson's ratio, yield strength, and strain-hardening characteristics also can be determined easily from this testing. Since CFWHCP is an anisotropic materials (composite materials), biaxial tensile testing is required [14].

Compression test is performed to determine the behavior of materials under crushing loads. The specimen is compressed and deformation at various loads is recorded. Compressive stress and strain are calculated and plotted as a stress-strain diagram which is used to determine elastic limit, proportional limit, yield point, yield strength and, for some materials, compressive strength [15].

2.6 CFRP IN OIL & GAS ENGINEERING APPLICATION

Carbon-fiber-reinforced polymer (CFRP) has become a notable material in structural engineering applications. Its use in industry can be either for retrofitting to strengthen an existing structure or as an alternative reinforcing material. CFRP could be used as pre-stressing materials due to their high strength. The advantages of CFRP over steel as a pre-stressing material, namely its light weight and corrosion resistance, should enable the material to be used for niche applications such as in offshore environments.

A research on Reinforced Composite Piping Technology found that fiber-reinforced polymer are better than steel in terms of the weight which is lighter, able to withstand high internal pressures, good corrosion resistance, impact resistance and torsion stiffness, lower life cycle cost, have smooth surface and better dimensional stability over temperature fluctuations [16]. It is proved that FRPs are better in terms of corrosion resistance as compared to steel where an experience from an oil company's used FRP pipes in low pressure water injection networks at offshore installations outside the coast of Africa finds that there are no signs of corrosion detected with Glass FRP pipes 12 after 2 years whereas the first holes were observed after approximately 6 months with carbon steel [17].

Candidate materials for tubular for West Kuwait oil fields including three FRPs - phenolic, vinyl ester and epoxy resin; two steels - N-80 and L-80 steels were tested for Microbially Influenced Corrosion (MIC) attack at high salt concentrations. All steel coupons were attacked. There was no evidence of attack of the vinyl ester or epoxy based FRP coupons by microorganisms. The surface gel coat of the vinyl ester and epoxy materials did not change in appearance and was not attacked or damaged by the bacteria. This shows FRP tubular performed better than those from low alloy steels [18].

Weight reduction is one of the major reason steel pipes are changed to with FRP pipes for the increasing application of FRP pipes in oil and gas industry. Several investigations made had shown that the use of FRP pipes generally reduces the weight in the range of 50-60%. In some cases, weight savings can even reach up to 80%. However, the weight savings obtained is very much depends on the design of the pipe system, working conditions and the pipe dimensions. An analysis of total weight/installed costs for Glass FRP and stainless steel has been made for selected parts of the sea water system on the Gullfaks A platform. Comparison of results for Glass FRP pipes and high molybdenum alloyed stainless steel indicated a weight savings for GRP of about 50 % for the selected part [17].

Carbon fiber reinforced composite (CFRP) is also found to be ideally suitable material for deep ocean applications. CFRP specimens when exposed at four depths namely 500, 1200, 3500, 4800 and 5100 m depths for 174 days did not lost in weight from weight loss measurement [19]. Ultimate tensile strength from tensile test result for exposed specimens is compared with control specimens. Tensile modulus data showed no significant variation in property compared to control specimens. Compressive strength of exposed specimens was also compared with control specimens. Flexure strength is also not affected by deep sea exposure. Inter-lamellar shear strength also had not undergone any change. All the facts clearly proved that deep-sea environment cannot affect the fiber/matrix interface.

CFRP had not undergone any change in property even after exposure in deepwater with temperature test as high as 150°C. It is proved from scanning electron microscope (SEM) observations that fiber pull-out and fiber-matrix interface failure were not seen. Microbiological observations revealed that bio-film formation on composite surface was not observed at all depth levels studied. It can be concluded that carbon fiber reinforced composite is a suitable material for deepwater applications through all the observation results obtained.

2.7 PAST RESEARCH ON QUASI-STATIC TEST

Based on the research of “A study on crushing behaviors of composite circular tubes with different reinforcing fibers” by Jung-Seok Kim, Hyuk-Jin Yoon, Kwang-Bok Shin [20], seven different kinds of circular tubes separately UD carbon/epoxy, UD Kevlar/epoxy, UD carbon-Kevlar/epoxy, UD Kevlar-carbon/epoxy, PW carbon/epoxy, PW Kevlar/epoxy and PW carbon-Kevlar/epoxy were fabricated. Quasi-static crushing tests were performed using a 100kN capacity hydraulic loading machine. All tubes were compressed until the load increased rapidly by stacking of debris inside them at loading rate of 10mm/min. During the tests, the load-displacement data was recorded as a function of time at intervals of 0.1s. Five replicated tests were carried out [20].

Based on the research of “Failure mechanism of woven natural silk/epoxy rectangular composite tubes under axial quasi-static crushing test using trigger mechanism” by R.A. Eshkoo a, A.U. Ude a, S.A. Oshkovr et al [21], three sample of square woven silk fiber tube were fabricated separated at different height of 50mm, 80mm and 120mm respectively. Widths of all side are fixed at 80mm. An automated Instron MTS 810 universal testing machine with a 250 KN loading capacity was used for the quasi-static compressive test of tubes. A constant cross head speed of 20mm/min was maintained throughout the test [21].

Result of quasi static loading in axial position of all the samples mentioned in 2 researches above will be compare accordingly to CFWHCP samples in result analysis section 3.2.5

CHAPTER 3

METHODOLOGY

3.1 PROJECT PROCESS FLOW

Figure 14 shows the designed project flow that has been followed along whole FYP progress. The main objective of this flow chart is to make sure the project schedule is keep on track throughout the semester to avoid any delay during progress. The chart flow give a rough idea on the studies involved, objective of interest, types of constant variables, fabrication of sample specimens, types of designed testing experiments and types of results analysis of interest.

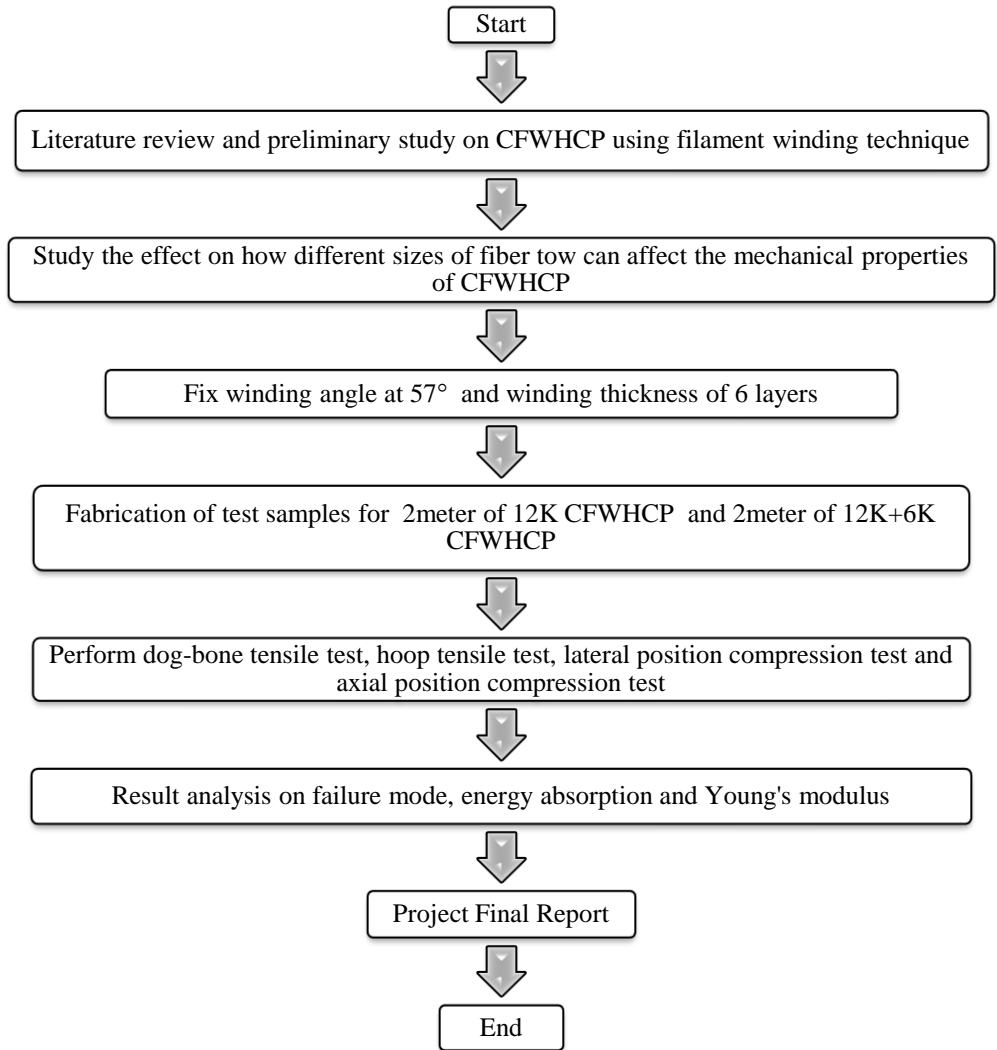


Figure 14: Project Process Flow Chart

3.2 RESEARCH METHODOLOGY

3.2.1 Preliminary Research Work

In this stage, data related to the project including material background research, journal studies, technical papers, past research studies and articles was collected. All information are gathered and compiled to have a better understanding towards the project. Meeting with the supervisor are also done weekly to have a better overview regarding the project that will be done including recommendations suggested by the supervisor.

3.2.2 Fabrication of sample specimens

In this project, 2 samples of carbon fiber wind to HDPE composite pipe (CFWHCP) were fabricated. Both of the samples are having 57° as the winding angle and 6 layers as the winding thickness. 2 HDPE composite pipes with length of 2 meter each were used for each sample respectively. CFWHCP were produced by using filament winding machine in SIRIM Permatang Pauh.

Sample 1:

2m HDPE composite pipe wind with only six 12K fiber tows

Sample 2:

2m HDPE composite pipe wind with mixture of four 6K and two 12K fiber tow

3.2.3 Fabrication of special jig

In this project, a few special jigs has been designed and fabricated to aid the cutting process. Refer technical drawing for all jigs in appendix section. The jigs are as follows:

i. Holder jig

Jig in figure 15 act as a holder to support CFWHCP while it is being rotated and cut into shorter section. Fabrication process is done using lathe machine.



Figure 15: Holder jig

ii. Straightener jig

Jig in figure 16 will be used to clamp CFWHCP to force it straight while it is being cut into shorter section. This is because the finish product of CFWHCP is not 100% straight due to the original shape of HDPE pipe (donut-like winding pattern). Fabrication process is done by using lathe machine and welding tools.



Figure 16: Straightener jig

iii. Hoop internal jig

Jig in figure 17 will be place inside hoop-shape CFWHCP during hoop tensile test. This is to ensure that during the tensile test, the stretching force will be transfer uniformly to every part of the specimen. Fabrication process is done using lathe and drilling machine.



Figure 17: Hoop internal jig

iv. Hoop external jig

Jig in figure 18 will be used to support the hoop internal jig located inside hoop-shape CFWHCP during hoop tensile test. This is to ensure that during the tensile test, the stretching force will be transfer uniformly to every part of the specimen. Fabrication process is done using drilling machine and welding tools.



Figure 18: Hoop external jig

3.2.4 Quasi-Static Lab Experiments

Following sample specimens will be fabricated from each sample 1 & sample 2 of CFWHCP fabricated in SIRIM Permatang Pauh.

- Dog-bone shape 3 pieces for tensile test
- Hoop shape 3 pieces for tensile test
- Original shape 90mm 4 pieces for axial compression test
- Original shape 90mm 4 pieces for lateral compression test

*Refer appendix for labeled technical drawing.

All of the specimens are complied with:

- ASTM D638/D2290 Standard for tensile test
- ASTM D695 Standard for compression test
- Thin cylinder spec which outer diameter-to-thickness ratio > 10

Pre-quasi static SEM result:

SEM test is being done to prove the hypothesis that there exists no fiber triangle void content before the carbon fiber is being enhanced with various sizes of fiber tow. Point of interest is the edge of carbon fiber which under microscope can clearly shows the overlapping arrangement of fiber tow which is where the no fiber triangle void content appears.

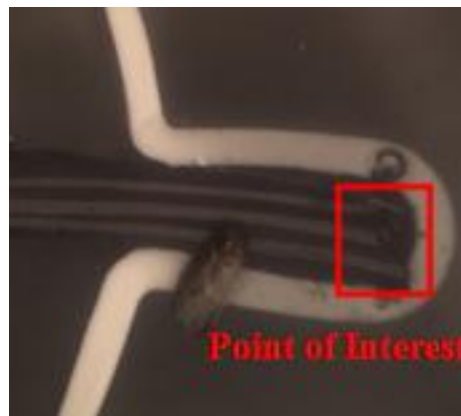


Figure 19: CFWHCP sample for SEM test

Figure 20 shows image of 12K fiber tow arrangement under microscope of 500x zoom in. It proved that no fiber triangle void is smaller as compare to 12K + 6K fiber tows which has lesser fiber tows involved when compare to figure 21.

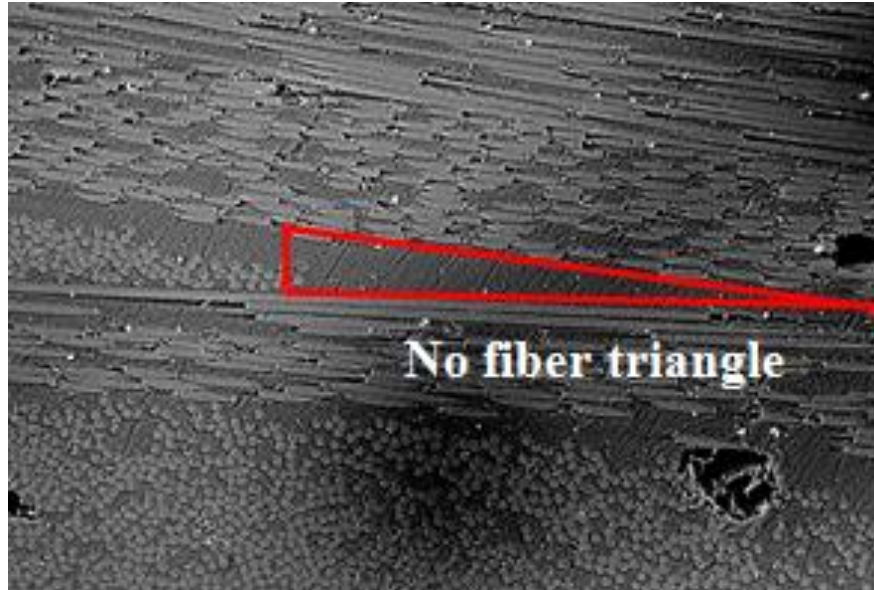


Figure 20: SEM result for six 12K fiber tows arrangement

Figure 21 shows image of 12K fiber tow with 6K fiber tow under microscope of 500x zoom in. It proved that no fiber triangle void content has been significantly increased as expected. This proved that the arrangement properties of CFWHCP has been reduced which will results in the weaken performance of mechanical properties such as tolerance towards failure mode, impact resistance and energy absorption.

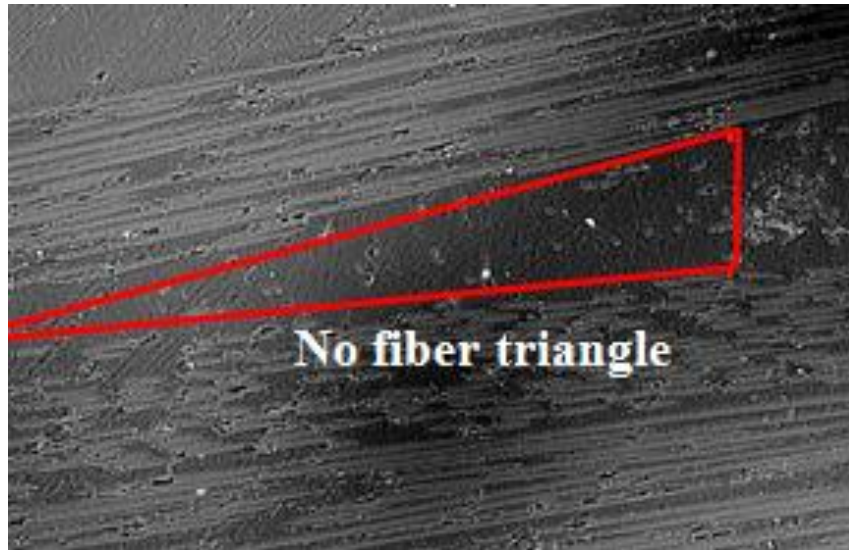


Figure 21: SEM result for two 12K + four 6K fiber tows arrangement

Table 1 shows the tabulated data for the average height of no fiber triangle void content calculated through 3 samples each for 12K and 12K+6K fiber tow. As calculated from the data of average height, the use of only 12K fiber tow has successfully reduced the height of no fiber triangle void content up to 53.3%.

Sample	Average Height (m)
12K	1.26E-08
12K + 6K	2.70E-08

Percentage of Reduction (%):
 $(2.70E-08 - 1.26E-08) / 2.70E-08 = 53.3\%$

Table 1: Result for SEM test

Re-boring of sample specimens into thin-cylinder spec:

In order for a hoop-shaped cylinder to be quality as thin-walled cylinder for tensile test, the requirement is that the outer diameter-to-thickness ratio must be more than 10.

Original outer diameter-to-thickness ratio :

$$66 / 8 = 8.25 \rightarrow \text{NOT QUALIFIED}$$

Re-boring process is then being introduced to the sample specimen to reduce the thickness of the cylinder. Figure 23 shows the picture of before and after re-boring process.

New outer diameter-to-thickness ratio :

$$66 / 6 = 11 \rightarrow \text{QUALIFIED}$$

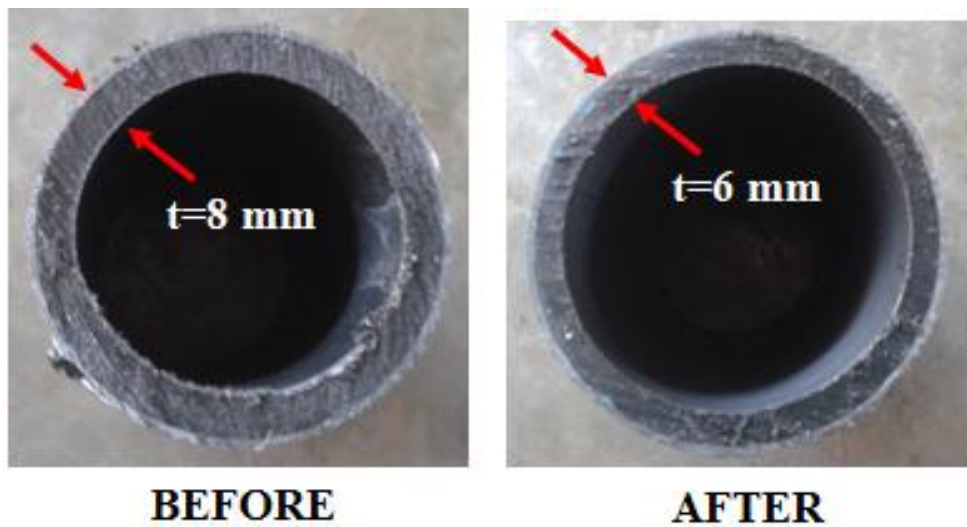


Figure 22: Before & after boring process

Quasi static loading experiments will be divided into 4 testing:

i. Tensile Test (Dog-bone shape):

- Dog-bone shape specimens are fabricated according to ASTM Standard
- Specimens are subjected to pulling speed of 20mm/min until failure
- Experiment are repeated 3 times to increase accuracy of results
- Stress-strain curve is then plotted and study the results to determine modulus of elasticity and maximum tension to failure

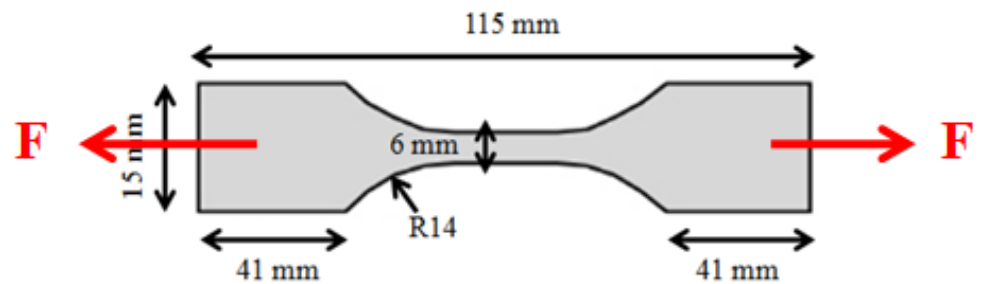


Figure 23: Dog-bones shape specimen for tensile test

ii. Tensile Test (Hoop shape):

- Hoop shape specimens are fabricated according to ASTM Standard
- Specimens are subjected to pulling speed of 20mm/min until failure
- Experiment are repeated 3 times to increase accuracy of results
- Stress-strain curve is then plotted and study the results to determine modulus of elasticity and maximum tension to failure

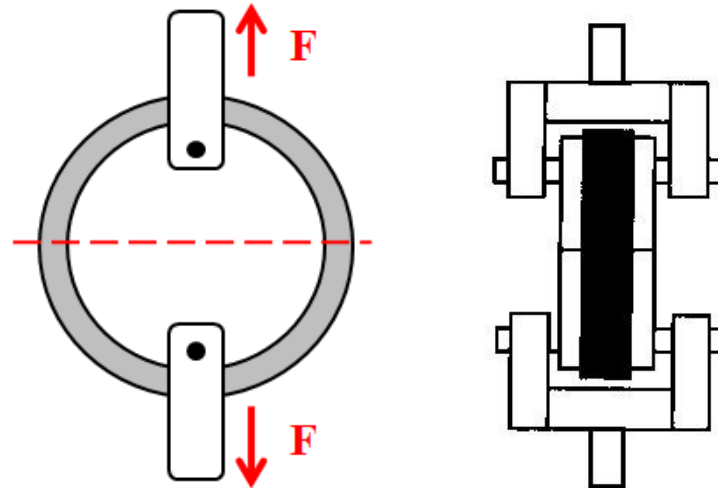


Figure 24: O-ring shape specimen for tensile test

iii. Crushing Test (Lateral Position):

- 90mm of CFWHCP specimens are placed in lateral position
- Specimens are subjected to compression speed of 20mm/min until failure
- Experiment are repeated 3 times to increase accuracy of results
- Load-displacement curve is then plotted and study the results to determine energy absorption and maximum load to failure

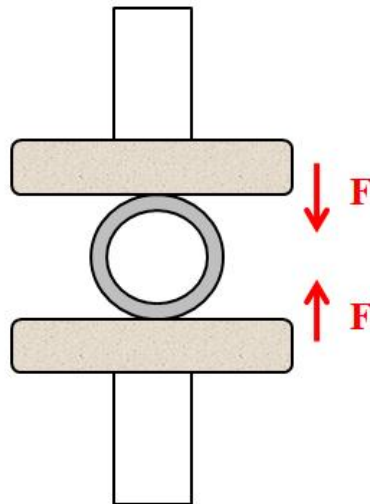


Figure 25: Original pipe specimen in axial position for compression test

iv. Crushing Test (Axial Position):

- 90mm of CFWHCP specimens are placed in axial position
- Specimens are subjected to compression speed of 20mm/min until failure
- Experiment are repeated 3 times to increase accuracy of results
- Load-displacement curve is then plotted and study the results to determine energy absorption and maximum load to failure

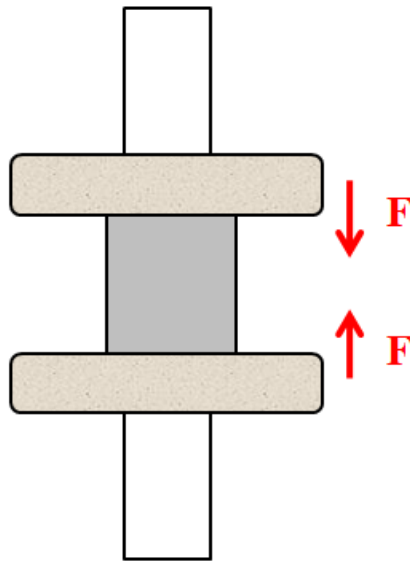


Figure 26: Original pipe specimen in lateral position for compression test

3.2.5 Results and Data analysis

i. Dog-boned Tensile Test

Original length of specimens → 115 mm

Sample	Failure Mode	Final Length	Max. Load	Young's Modulus
12Kx2 + 6Kx4	<ul style="list-style-type: none"> Carbon fiber broke within 3 seconds Very brittle for carbon fiber layer, surface of failure is even without much resistance towards pulling force 	130 mm	578.73kN	1609MPa
12Kx6	<ul style="list-style-type: none"> Carbon fiber can resist the pulling force and broke after 3 seconds Brittle for carbon fiber layer, surface of failure is not even, able to see some resistance before the sample breaks 	130 mm	764.73kN	19592MPa

Table 2: Results for dog-boned tensile test

Figure 27 shows the top view of 12K+6K (top) and 12K (bottom) samples after dog-boned tensile test. 12K+6K sample shows a straight line of even surface breakage while 12K sample shows uneven surface breakage. This is due to the stronger 12K sample able to resist the pulling force more as compare to 12K+6K sample.



Figure 27: Dog-bone tensile sample

Figure 28 shows the stress-strain curve of 12K sample versus 12K+6K sample in dog-boned tensile test. Result clearly shows that 12K sample require higher stress value in order to reach its failure point as compare to 12K+6K sample which contributed to higher Young's modulus value as recorded in table 2. The graph also shows that 12K sample can tolerate with much higher stress before it eventually failed as compare to 12K+6K sample.

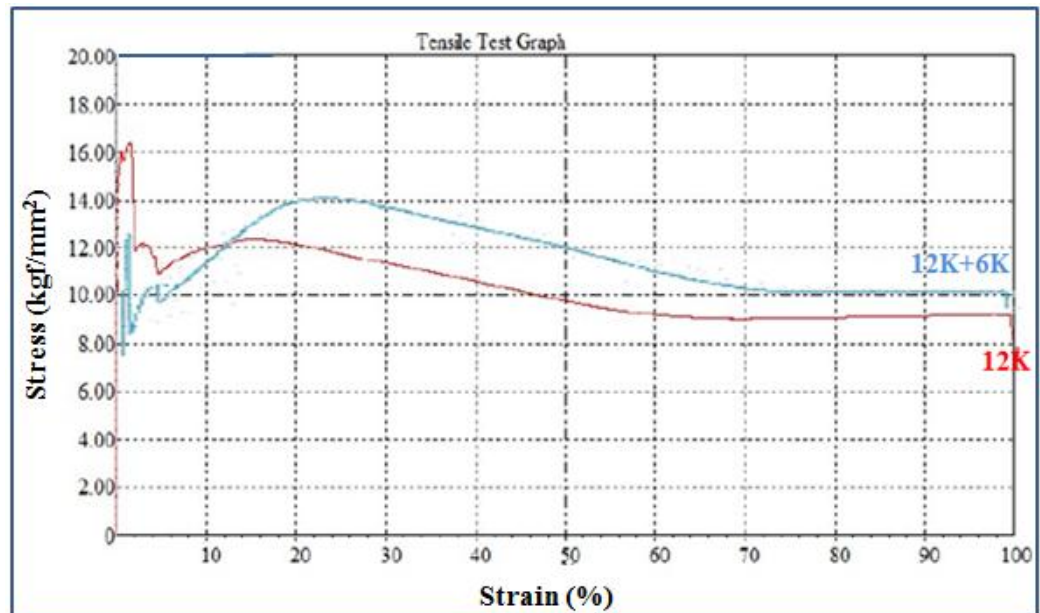


Figure 28: Dog-bone tensile stress-strain graph

ii. Hoop Tensile Test

Original length of specimen → 66 mm

Sample	Failure Mode	Final Length	Max. Load	Young's Modulus
12Kx2 + 6Kx4	<ul style="list-style-type: none"> • HDPE layer broke together with carbon fiber layer • Very brittle for carbon fiber layer, surface of failure is even without much resistance towards pulling force 	66 mm	4.56kN	5.5MPa
12Kx6	<ul style="list-style-type: none"> • HDPE layer only necking when the carbon fiber layer broke • Brittle for carbon fiber layer, surface of failure is not even, able to see some resistance before the sample breaks 	66 mm	11.53kN	36.25MPa

Table 3: Results for hoop tensile test

Figure 29 shows the top view of 12K+6K (top) and 12K (bottom) samples after hoop tensile test. 12K+6K sample shows a straight line of even surface breakage while 12K sample shows uneven surface breakage. This is due to the stronger 12K sample able to resist the pulling force more as compare to 12K+6K sample.

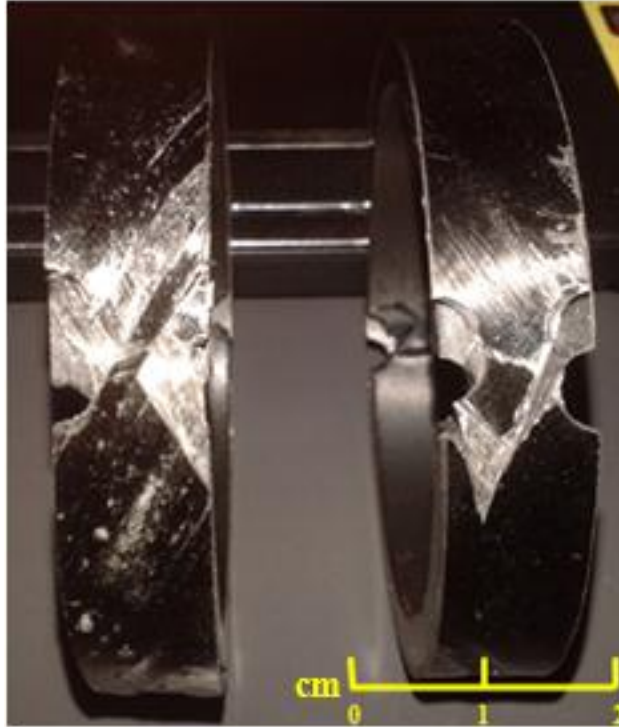


Figure 29: Hoop tensile sample

Figure 30 shows the stress-strain curve of 12K sample versus 12K+6K sample in hoop tensile test. Result clearly shows that 12K sample has steeper curve profile as compare to 12K+6K sample which contributed to higher Young's modulus value as recorded in table 3. The graph also shows that 12K sample can tolerate with much higher stress before it eventually failed as compare to 12K+6K sample.

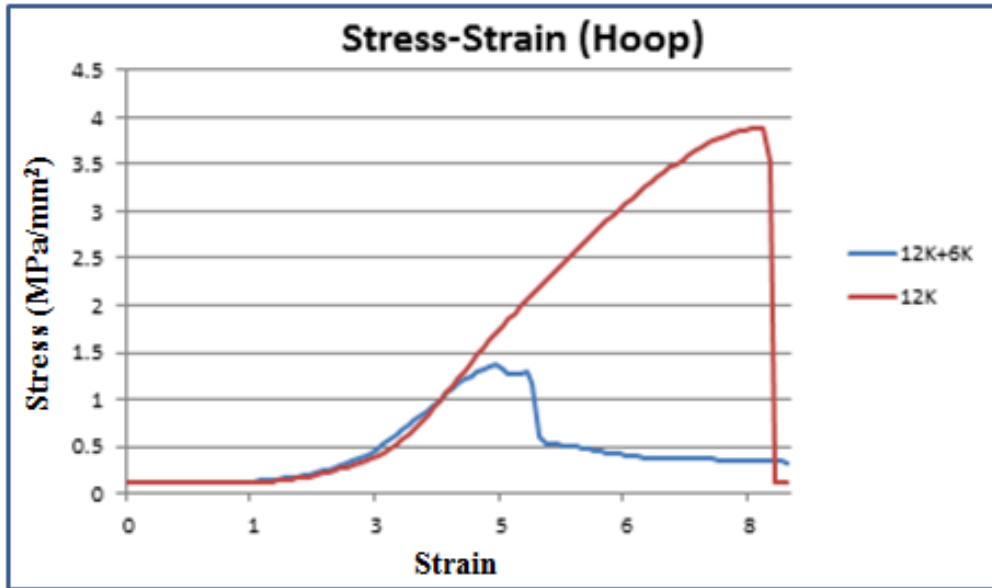


Figure 30: Hoop tensile Stress-Strain graph

iii. Quasi Static Compression Test (Axial Position)

Original height of specimen → 90 mm

Sample	Failure Mode	Final Height	Max. Load	Energy Absorption
12Kx2 + 6Kx4	<ul style="list-style-type: none"> Multiple cracks on the surface of specimens Severe dent on carbon fiber surface and the inner surface of HDPE pipe 	79 mm	37.78kN	99E6kJNm
12Kx6	<ul style="list-style-type: none"> No crack appear on the surface of specimens Only slight dent on carbon fiber surface and the inner surface of HDPE pipe 	82 mm	43.13kN	113E6kJNm

Table 4: Results for quasi static compression test (axial position)

Figure 31 shows the top view of 12K+6K (right) and 12K (left) samples after axial position compression test. 12K+6K sample shows severe crack while 12K sample only shows minor dented marks. This is due to the stronger 12K sample able to resist the compression force more as compare to 12K+6K sample.



Figure 31: top view (axial position compression test)

Figure 32 shows the side view of 12K+6K (right) and 12K (left) samples after axial position compression test. 12K+6K sample shows severe crack on overall outer surface while 12K sample only shows minor dented line at the middle part of sample. This is due to the stronger 12K sample able to resist the compression force more as compare to 12K+6K sample.

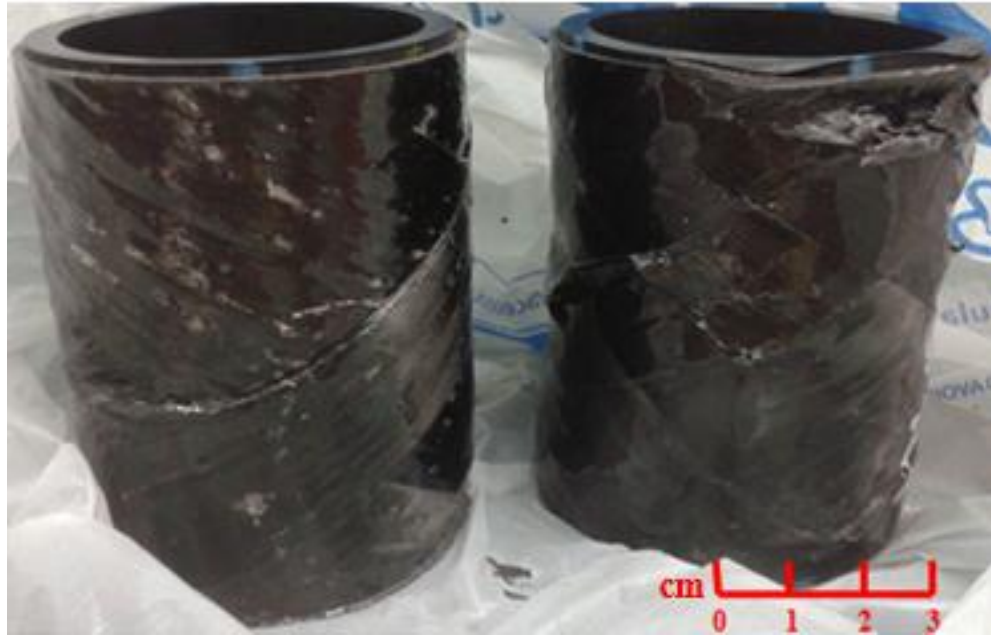


Figure 32: side view (axial position compression test)

Figure 33 shows the load-displacement curve of 12K sample versus 12K+6K sample in axial position compression test. Result clearly shows that 12K sample has larger area under the curve profile as compare to 12K+6K sample which contributed to higher energy absorption value as recorded in table 4. The graph also shows that 12K sample can tolerate with much higher load before it eventually failed as compare to 12K+6K sample. Pictures in figure 33 shows the shape of the sample for both 12K+6K and 12K when completely fail during axial compression test. It is clearly seen that sides of both sample folded inwards in shape when they reached their failing point.

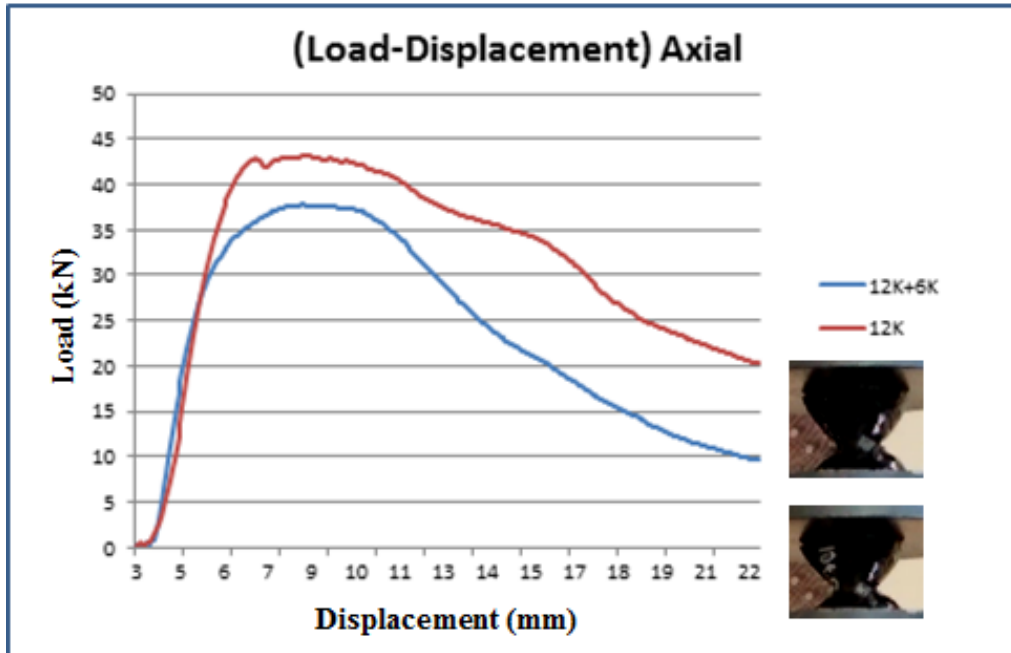


Figure 33: Axial compression test load-displacement graph

Figure 34 shows the comparison of peak load required to fail the samples between the samples mentioned in earlier literature review and CFWHCP samples. Comparison result shows that CFWHCP 12K which the void has been reduced shows the highest peak load among all the other samples. This also proved that CFWHCP 12K sample has the high strength to able to endure the compression force being introduced during quasi static compression test. Hypothesis is thus proven that the size of no fiber triangle void content and the mechanical properties of that material are inversely proportional to each other. By reducing the size of no fiber triangle void content, the mechanical properties of that respective material can be enhanced effectively.

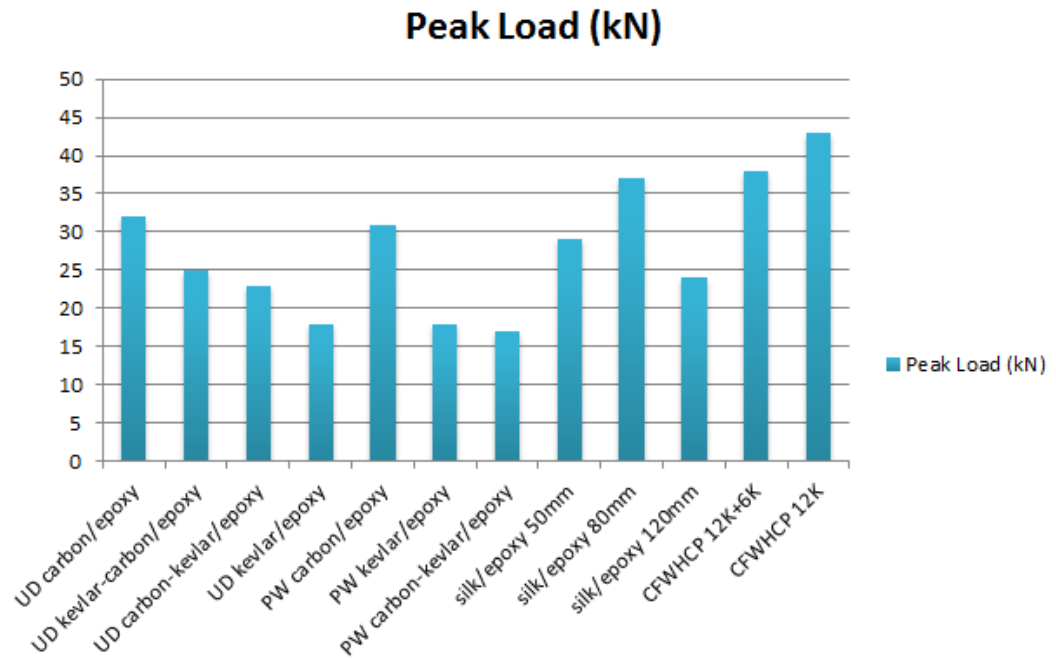


Figure 34: Peak load comparison with past research samples

iv. Quasi Static Compression Test (Lateral Position)

Original height of specimen → 66 mm

Sample	Failure Mode	Final Height	Max. Load	Energy Absorption
12Kx2 + 6Kx4	<ul style="list-style-type: none"> Multiple cracks on the surface of specimens Slight dented mark on the inner surface of HDPE pipe 	53 mm	5.91kN	69E6kNm
12Kx6	<ul style="list-style-type: none"> No crack appear on the surface of specimens No dented mark the inner surface of HDPE pipe 	57 mm	7.97kN	87E6kNm

Table 5: Results for quasi static compression test (lateral position)

Figure 35 shows the top view of 12K+6K (right) and 12K (left) samples after lateral position compression test. 12K+6K sample shows permanent folded mark on side while 12K sample does not shows any folded mark on the side. This is due to the stronger 12K sample able to resist the compression force more as compare to 12K+6K sample.

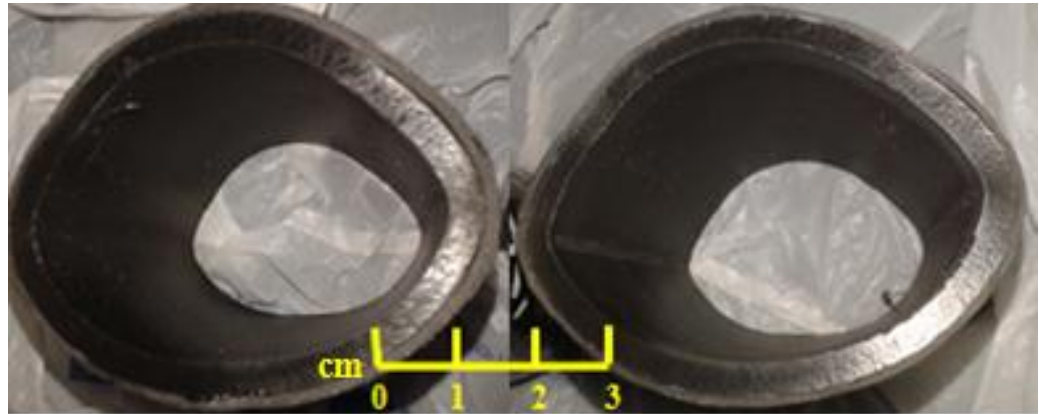


Figure 35: top view (lateral position compression test)

Figure 36 shows the side view of 12K+6K (right) and 12K (left) samples after lateral position compression test. 12K+6K sample shows severe cracks at the middle part of sample while 12K sample does not shows any crack mark on the side. This is due to the stronger 12K sample able to resist the compression force more as compare to 12K+6K sample.



Figure 36: side view (lateral position compression test)

Figure 37 shows the load-displacement curve of 12K sample versus 12K+6K sample in lateral position compression test. Result clearly shows that 12K sample has larger area under the curve profile as compare to 12K+6K sample which contributed to higher energy absorption value as recorded in table 5. The graph also shows that 12K sample can tolerate with much higher load before it eventually failed as compare to 12K+6K sample. Pictures in figure 37 shows the shape of the sample for both 12K+6K and 12K when completely fail during lateral compression test. It is clearly seen that for both sample, top side folded inwards and sides folded outwards in shape when they reached their failing point.

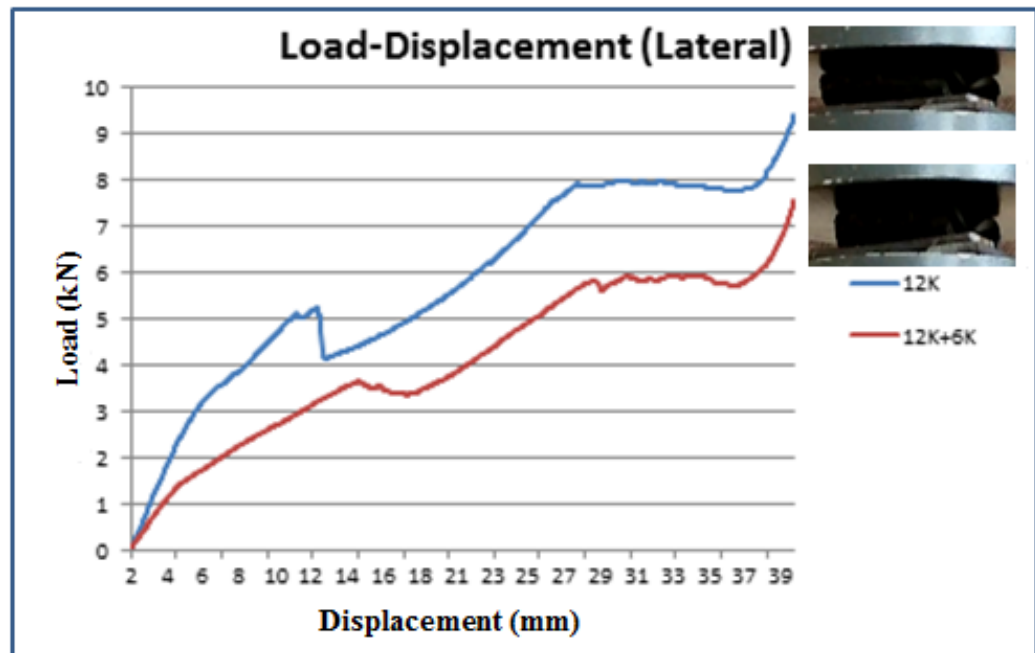
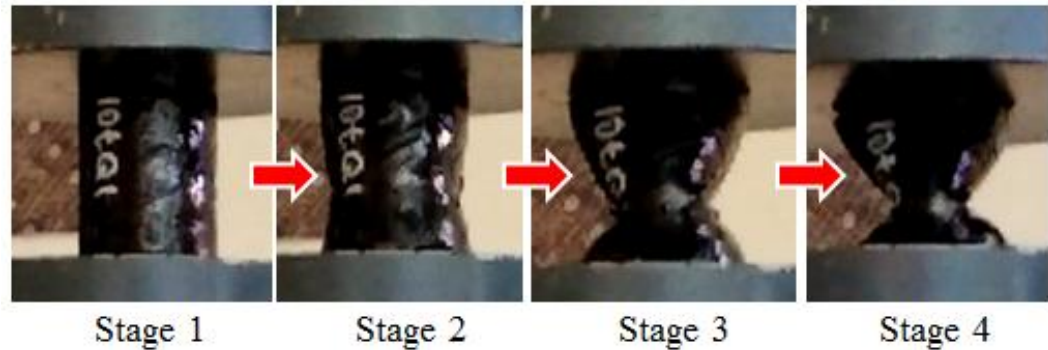


Figure 37: Lateral compression test load-displacement graph

3.2.6 Axial Compression Stages



Stage 1

Both end of sample starts to experience axial compression force. It starts to transfer the load force from both ends towards the center part of the sample.

Stage 2

Compression force at both ends of the sample reached maximum and eventually center part of the sample start to experience deformation in shape. “Crack” sound started to appear as it signifies the outer layer of carbon fiber started to break.

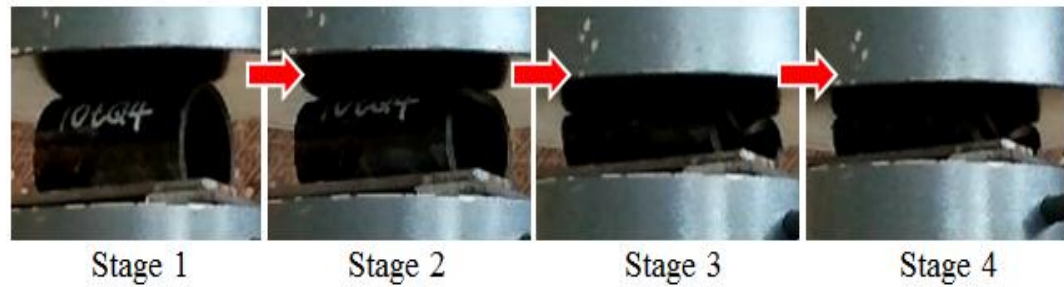
Stage 3

“Crack” sound frequency increases signify more and more fiber fails and break at the outer layer. Load force starts to be transferred from outer layer of carbon fiber towards inner layer of HDPE composite pipe.

Stage 4

At this final stage, the outer layer of carbon fiber experience cracks and defragmentation until eventually fails. HDPE composite pipe at inner layer continue to experience the load force until eventually deformed and exceeds its elastic limits.

3.2.7 Lateral Compression Stages



Stage 1

Both top and bottom side of sample starts to experience lateral compression force. It starts to transfer the load force from both ends towards the center part of the sample.

Stage 2

Compression force at top and bottom side of the sample reached maximum and eventually top center part of the sample start to experience minor fold in shape. “Crack” sound started to appear as it signifies the outer layer of carbon fiber started to break.

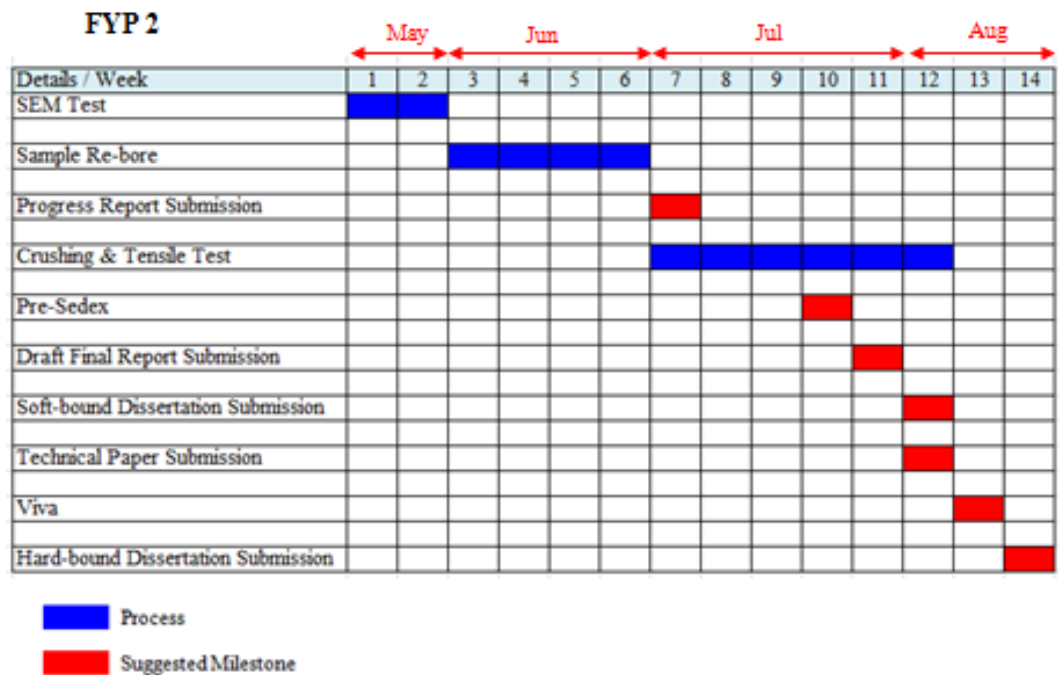
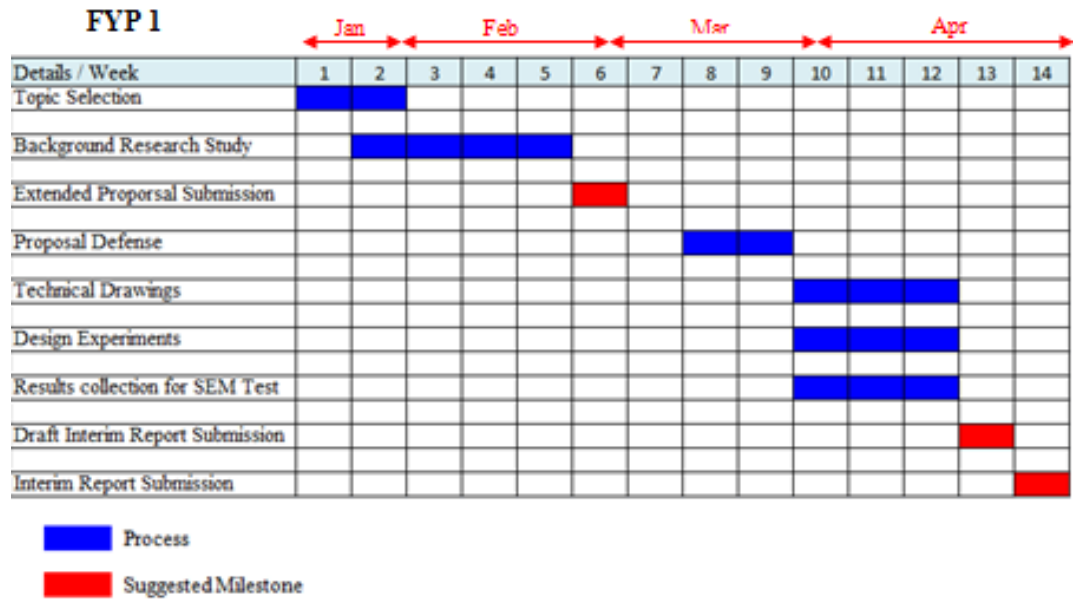
Stage 3

“Crack” sound frequency increases as the fold shape at the top center part become more obvious. Side surface of the sample also experience deformation in shape when the folding process took place. Folded marks and crack defragmentation marks can be seen as the compression force continue to be experience by the sample

Stage 4

At this final stage, the whole sample experience total fails. Deformation that took place is permanent as the sample already exceeds compression force which exceeds its elastic limits.

3.3 GANTT CHART & KEY MILESTONE



CHAPTER 4

CONCLUSION & RECOMMENDATION

4.1 CONCLUSION

As conclusion, the summary of the project is as follow:

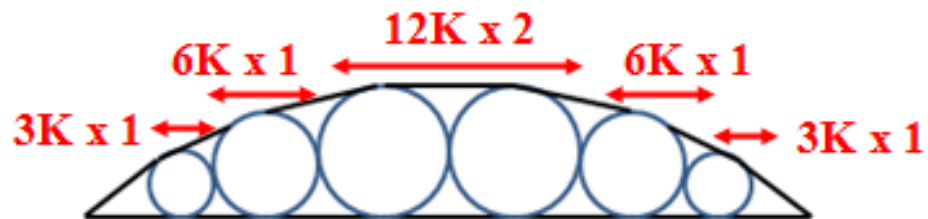
1. First objective which is to investigate how different sizes of carbon fiber tow arrangement winding on high density polyethylene pipe can affect the level of enhancement of mechanical properties on the composite pipe is achieved through the results of SEM test.
 - It proved that same sizes of carbon fiber tow arrangement can increase the mechanical properties of CFWHCP by reducing the sizes of no fiber potential triangle void
 - 12K+6K sample has average height of void of $2.70E-08m$ compare to 12K sample at $1.26E-8$
2. Second objective which is to study impact of quasi static axial loading on carbon fiber wind to high density polyethylene composite pipe (CFWHCP) is achieved through results of tensile and quasi-static compression test. It proved that sample of CFWHCP which same sizes of carbon fiber tows provide enhanced mechanical properties.
 - In dog-boned tensile test, 12K sample has higher Young's modulus which is $19592MPa$ as compare to 12K+6K sample at $4606MPa$
 - In hoop tensile test, 12K sample has higher Young's modulus which is $36.25MPa$ as compare to 12K+6K sample at $5.5MPa$
 - In axial compression test, 12K sample has higher energy absorption which is $113E6kJm$ as compare to 12K+6K sample at $99E6kJm$

- In lateral compression test, 12K sample has higher energy absorption which is 87E6kNm as compare to 12K+6K sample at 69E6kNm
- 12K sample has up to 60% increment in energy absorption compare to PW carbon-Kevlar/epoxy sample and up to 44% compare to silk/epoxy 120mm sample in quasi static axial loading test

4.2 RECOMMENDATION

For recommendation, the author would like to propose:

1. Further research with CFWHCP which the HDPE is being polished with sandpaper before the winding process to make sure both layer has more adhesive force towards each other
2. Further research with CFWHCP of new fiber tow arrangement as follow:



- By replacing the outermost tow with even smaller size of 3K fiber instead of 6K, we could see that the no fiber triangle potential void has the tendency to reduced even further as compare to all 12K fiber

REFERENCES

- [1] F. Abdalla, S. Mutasher, Y. Khalid, S. Sapuan, A. Hamouda, B. Sahari, *et al.*, "Design and fabrication of low cost filament winding machine," *Materials & design*, vol. 28, pp. 234-239, 2007.
- [2] Martin Alberto Masuelli, "Fiber Reinforced Polymers - The Technology Applied for Concrete Repair," National University of San Luis, 2013.
- [3] Dr. Dmitri Kopeliovich, "Carbon Fiber Reinforced Polymer Composites," 2012.
- [4] B. BALYA, "Design And Analysis Of Filament Wound Composite Tubes," Middle East Technical University, 2004.
- [5] J. M. Starbuck and L. B. Cataquiz, "Evaluation of Large Tow-Size Carbon Fiber for Reducing the Cost of CNG Storage Tanks Society of Automotive Engineers, Inc.", 1998.
- [6] B. J. Yang, S. K. Ha, S. H. Pyo, and H. K. Lee, "Mechanical characteristics and strengthening effectiveness of random-chopped FRP composites containing air voids," *Composites Part B: Engineering*, vol. 62, pp. 159-166, 6// 2014.
- [7] Z. A-ying, Z. Dong-xing, L. Di-hong, S. Tao, X. Hai-ying, and J. Jin, "Tensile Strength of Hygrothermally Conditioned Carbon/Epoxy Composites with Voids," *Energy Procedia*, vol. 16, Part C, pp. 1737-1743, // 2012.
- [8] Jon Soller, "Choosing the Appropriate Resin," *Soller Composites*, 2004
- [9] David Cripps, "Epoxy Resins," 1985.
- [10] D. K. Roylance, "Netting analysis for filament-wound pressure vessels." USA: AMMRC TN 76-3, 1976.
- [11] Todd Johnson, "Filament Winding - The Basics," 2013.
- [12] Prof. Andrei M Reinhorn, "LOADING SYSTEMS: Static Structural Testing" *Lecture Series 5*; CIE616, 1990.

- [13] Czichos, Horst, "Springer Handbook of Materials Measurement Methods," Berlin: Springer. pp. 303–304. ISBN 978-3-540-20785-6. // 2006.
- [14] Davis, Joseph R., "Tensile testing (2nd ed.)". ASM International. ISBN 978-0-87170-806-9. // 2004.
- [15] *ASM Handbook, Vol. 8, Mechanical Testing and Evaluation*, ASM International, Materials Park, OH 44073-0002 // 2000.
- [16] C. I. Oseghale and N. Umeania, "Application of Reinforced Composite Piping (RCP) Technology to Liquefied Petroleum Gas Distribution," *Research Journal of Applied Sciences*, vol. 6, pp. 197-204, 2011.
- [17] R. Stokke, "Use Of Glass Fiber-Reinforced Plastics (Grp) In Seawater Pipe System Offshore," in *Offshore Technology Conference*, 1988.
- [18] P. Scott, A. Al-Hashem, and J. Carew, "Experiments on MIC of steel and FRP downhole tubulars in west Kuwait brines," *CORROSION 2007*, 2007.
- [19] R. Venkatesan, E. Dwarakadasa, and M. Ravindran, "Study on behavior of carbon fiber-reinforced composite for deep sea applications," in *Offshore Technology Conference, Houston, TX*, 2002.
- [20] Jung-Seok Kim, Hyuk-Jin Yoon , Kwang-Bok Shin, "A study on crushing behaviors of composite circular tubes with different reinforcing fibers," *International Journal of Impact Engineering* 38 (2011) 198-207, 2011.
- [21] R.A. Eshkoo a, A.U. Ude a, S.A. Oshkovr et al, "Failure mechanism of woven natural silk/epoxy rectangular composite tubes under axial quasi-static crushing test using trigger mechanism," *International Journal of Impact Engineering* 64 (2014) 53-61, 2013.
- [22] H.H.Ya, "Impact loading of composite plastic pipes," 2006.

APPENDIX